INSTITUTE OF PLASMA PHYSICS

NAGOYA UNIVERSITY

Deflagration Wave Formed by Ion Beam

Part II. In Spherical Target

T. Abe*, K. Kasuya*, K. Niu* and M. Tamba#

(Received June 22, 1979)

IPPJ-403 June 1979

RESEARCH REPORT

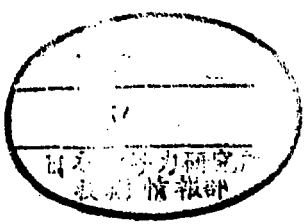

NAGOYA, JAPAN

Deflagration Wave Formed by Ion Beam

Part II. In Spherical Target

T. Abe*, K. Kasuya*, K. Niu* and M. Tamba#

(Received June 22, 1979)

IPPJ-403 June 1979

Further communication about this report is to be sent to the Research Information Center, Institute of Plasma Physics, Nagoya University, Nagoya, Japan.

---

* Permanent address: Tokyo Institute of Technology, Tokyo, Japan.

Permanent address: The Institute of Physical and Chemical Research, Wako-shi, Saitama, Japan.

Deflagration Wave Formed by Ion Beam

Part II. In Spherical Target

T. Abe*, K. Kasuya*, K. Niu* and M. Tamba#

* Tokyo Institute of Technology
Tokyo, Japan

The Institute of Physical and Chemical Research
Wako-shi, Saitama, Japan

Abstract

Analyses are given for structures of deflagration waves formed by ion beams in spherical targets. The singularity at the sonic point disappears in the spherical target if the beam pressure is in balance with the plasma pressure. The expanding supersonic flow of the background plasma can be connected with the subsonic flow in the core of the target through the deflagration wave. The length and the strength of the deflagration wave in the spherical target is comparable with the corresponding ones in the slab target.

§1. Introduction

In inertial-confinement fusion, the target is compressed by the accelerating deflagration wave which is formed by the action of the external energy driver.[1] As for the external energy driver, the laser is known to be useful. Recently, the other drivers such as REB and light-ion beam attract attentions.

In this paper, we analyse the deflagration wave which is formed when the ion beam impinges on the target. Our analytical model is developed with the following assumptions; 1) the target heated by the ion beam is already fully ionized and is treated by a fluid with one temperature, 2) the ion beam is also treated by a cold fluid, 3) the ion beam is already neutralized by electrons, 4) the number density of the beam is so small in comparison with that of the plasma as to neglect the backward flow of the beam after the release of the energy, 5) the deflagration wave is maintained in a stationary state, 6) the beam interacts with the plasma through the classical Coulomb scattering. The schematic diagram of this model is shown in Fig.1.

In the deflagration wave in the slab target, the sonic point is singular.[2] So the background plasma in the subsonic condition can not expand continuously through the deflagration wave into the supersonic region. This is the case for the deflagration wave supported by laser.[3] In inertial-confinement fusion, the pellet is spherical, and the spherically symmetric deflagration wave is formed. In this paper, we show

that the singularity at the sonic point in the slab model disappears in the spherically symmetric model, and the flow changes continuously from the subsonic to the supersonic region through the sonic point.

§2. Basic Equations

The basic equations in the spherical coordinate are as follows;

$$nur^2 = 1, \tag{1}$$

$$n_b u_b r^2 = -1, \tag{2}$$

$$nu\frac{du}{dr} + n_b u_b \frac{du_b}{dr} = -\frac{3}{5}\frac{dnT}{dr}, \tag{3}$$

$$u^2/2 - \alpha^3 \beta u_b^2/2 + 3T/2 = 2 - \alpha^3\beta/2, \tag{4}$$

$$\frac{du_b}{dr} = -\frac{\bar{r}_s}{\bar{\lambda}_s}\frac{n}{T^{3/2}}. \tag{5}$$

Here $\bar{n}$ is the number density, $\bar{r}$ the radius, $\bar{u}$ the velocity, $\bar{T}$ the temperature and the suffix b represents the quantities of the beam. The quantities except $\bar{u}$ are normalized by the respective quantities at the sonic point represented by the suffix s. The velocity $\bar{u}$ is normalized by the sonic speed $\bar{u}_s$ $(=\sqrt{(5/3)\bar{k}\bar{T}_s/\bar{m}_i})$ at the sonic point, where $\bar{m}_i$ and $\bar{m}_e$ are the ion and electron masses, respectively. The bars on the variables are omitted after they are normalized. In eq.(4), α and β are respectively the ratios of the velocity and the number density of the beam to those of the target plasma at

the sonic point;

$$\alpha = [-\bar{u}_b/\bar{u}]_s, \quad \beta = [\bar{n}_b/\bar{n}]_s.$$

In eq.(5), $\bar{\lambda}_s$ is the representative length of the interaction;

$$\bar{\lambda}_s = \frac{12\pi\sqrt{2}\alpha\bar{\varepsilon}_0^2\bar{T}_s^2}{\bar{e}^4\bar{n}_s \log\Lambda}\left(\frac{\bar{m}_i}{\bar{m}_e}\right)^{1/2},$$

where $\log\Lambda$ is the Coulomb logarithm, $\bar{\varepsilon}_0$ the dielectric constant in vacuum and $-\bar{e}$ the electron charge.

In order to solve eqs.(1)-(5), we employ the following boundary conditions at r=1.

$$u = T = n = 1, \quad u_b = -1. \tag{6}$$

Equations (1) and (2) are the mass conservation law for the target plasma and the beam. Equation (4) is the energy conservation law. Equation (3) is the total momentum conservation law for the background plasma and the beam, while eq.(5) is the momentum conservation law for the beam only. The right hand side of eq.(5) shows the mutual interaction between the background plasma and the beam.

The exact expression of the Coulomb interaction consists of the complicated terms including the error function.[4] Here, for simplicity, we use the approximate interaction term as the right hand side of eq.(5), assuming that the beam velocity is much smaller than the electron thermal velocity.

Let us define the front of the deflagration wave by the point where u_b=0. Then eq.(4) becomes

$$u_f^2 + 3T_f = 4 - \alpha^3\beta \ , \qquad (7)$$

where the suffix f means the quantities at the front. In order to satisfy the mass conservation (1), we must assume the existence of the source of plasma with T_f and n_f at the radius r_f. Since the left hand side of eq. (7) must always be positive, the condition $\alpha^3\beta<4$ must be satisfied. As can be seen from eq. (7), the total energy flux in the wave is equal to the sum of the energy flux (part I) of the plasma from the front and the energy flux (part II) of the beam from the sonic point. The condition $\alpha^3\beta=4$ means that the energy flux of part I can be neglected in comparison with that of part II. Namely, the total energy flux is supplied by the beam from the sonic point.

§3. Elimination of Singularity at Sonic Point

Substituting du_b/dr and $d(nT)/dr$ in eq. (3) from eqs. (1), (2), (4) and (5), we obtain the equation for du/dr;

$$\frac{du}{dr} = \left[-(5u^2\alpha^2\beta - 2\alpha^3\beta u u_b) \frac{\bar{r}_s}{\bar{\lambda}_s} \frac{1}{ur^2T^{3/2}} + 6\frac{uT}{r} \right] \frac{1}{u^2-T} \ . \qquad (8)$$

Since u=T=1 at r=1, eq. (8) is singular there unless the numerator does not equal to zero. However, when the numerator equals to zero, that is,

$$-(5\alpha^2\beta + 2\alpha^3\beta)\bar{r}_s/\bar{\lambda}_s + 6 = 0 \ , \qquad (9a)$$

this sigularity vanishes.

The terms in the right hand side of eq.(9a) represents the pressures. The first term originates in the beam and the second in the plasma in the spherical configuration. Therefore, eq.(9a) requires the balance of the two pressures. The balance determines the ratio $\bar{r}_s/\bar{\lambda}_s$ for given parameters α and β;

$$\frac{\bar{r}_s}{\bar{\lambda}_s} = \frac{6}{5\alpha^2\beta+2\alpha^3\beta} . \tag{9b}$$

To see the meaning of eq.(9b), we consider the deflagration waves with various intensities (various α and β), provided that the sonic state ($\bar{\lambda}_s$) is constant. As can be seen from the second term in the right hand side of eq.(8), the pressure caused by the spherical configuration is inversely proportional to the radius r. Under the balance of the two pressures, the radius $\bar{r}_s$ at the sonic point decreases as the intensity of the beam increases. Equation (9b) clearly shows that $\bar{r}_s$ becomes small when α and β increases.

The gradient of u at the sonic point is evaluated as;

$$\left[\frac{du}{dr}\right]_{r=1} = \lim_{r\to 1} \frac{d}{dr}\left[-(5u^2\alpha^2\beta-2\alpha^2\beta u u_b)\frac{\bar{r}_s}{\bar{\lambda}_s}\frac{1}{ur^2T^{3/2}}\right.$$

$$\left.+6\frac{uT}{r}\right] / \left[\frac{d}{dr}(u^2-T)\right]. \tag{8'}$$

By using eqs.(1)-(5), eq.(8') reduces to

$$8q^2+q[k(5\eta-2\xi)+4]+2\xi k^2-10\xi k-6 = 0. \tag{10}$$

where $q=[du/dr]_{r=1}$, $\eta=\alpha^2\beta$, $\xi=\alpha^3\beta$, and $k=\bar{r}_s/\bar{\lambda}_s$. The two solutions of eq.(10) correspond to the two different flows of the background

plasma at the sonic point. The positive solution gives the flow which changes from the subsonic to the supersonic state at the sonic point. The negative solution gives the flow which changes from the supersonic to the subsonic state. Through the deflaration wave as is considered here, the flow must change from the subsonic to supersonic state. So that, we must choose the positive solution.

The steady deflagration wave can exist under restricted conditions. Let us first examine the case that eq.(10) has two solutions with the opposite signs. Then the following condition must be satisfied;

$$\xi k^2 - 5\xi k - 3 < 0. \tag{11}$$

On the other hand, eq.(9b) for k ($=\bar{r}_s/\bar{\lambda}_s$) can be rewritten as;

$$k = \frac{1}{\xi}\,\frac{6}{5\eta/\xi+2} = \frac{c}{\xi}\,, \tag{12}$$

where c is restricted into

$$6/7<c<3$$

since we expect to be

$$0<\frac{\eta}{\xi} = \frac{1}{\alpha} = \left[-\frac{u}{u_b}\right]_s < 1.$$

Substituting k from eq.(12) into eq.(11), we get an inequality for ξ ($= \alpha^3\beta$);

$$\frac{c^2}{5c+3} < \xi \tag{13}$$

The left hand side of eq.(13) increases from 0.1 to 0.5 with c. When ξ is smaller than 0.1 , eq.(10) has two positive, or

two negative or two complex solutions. If β is small (and hence ξ is small), r_s (k) becomes large as can be seen from eq. (9b). In such a case, the solution is physically meaningless. In our analysis, the numerical integrations of eqs.(5) and (8) with the boundary condition (6) are performed by using Runge-Kutta-Gill method for ξ which satisfies the condition (13).

§4. Spherical Deflagration Wave

Numerical integrations lead to n_f, T_f, u_f, $n(r)$, $u(r)$, $T(r)$, and $u_b(r)$. The dimensional values $\bar{n}(\bar{r})$, $\bar{u}(\bar{r})$, $\bar{T}(\bar{r})$, $\bar{n}_b(\bar{r})$ and $\bar{u}_b(\bar{r})$ are obtained if we specify $\bar{n}_f$ and $\bar{T}_f$ in addition to α and β. Equation (9b) determines $\bar{r}_s$ and hence $\bar{r}_f$. The structure of the deflagration wave is plotted in Fig.2; the temperature in Fig.2a, the velocity in Fig.2b and the beam velocity in Fig.2c. As can be seen from Fig.2c, the beam which enters into the background plasma, interacts with the plasma, reduces the speed, and stops at $r=r_f$. Figures 2a and 2b show that the background plasma with n_f and T_f at r_f flows out, being heated and accelerated. Outside of the sonic point, the plasma expands and is cooled. In the region between the front (r_f) and the sonic point ($r_s=1$), the main part of the beam energy is deposited. We call this region the deflagration wave. The small part of the beam energy is deposited in the expanding supersonic region of the background plasma. Figure 3 shows the ratio of the beam velocity at the sonic point to that at the infinite point. This ratio is not so small and depends

on the details of the interaction between the beam and the plasma. The length of the deflagration wave is about λ_s as can be seen from Fig.4 and is comparable with that in slab target.[2] The strength of the deflagration wave ($\bar{n}_f/\bar{n}_f$ and $\bar{T}_s/\bar{T}_f$) is shown in Fig.5. The abscissa is the ratio between the energy flux of the background plasma and that of the beam. For comparison, corresponding values in the slab target are also plotted in the figures by dotted lines.

§5. Conclusion

In this paper, the structures are analysed for the deflagration waves formed by ion beams in the spherical targets. It is very peculiar in the spherical configuration that the deflagration wave can connect the subsonic plasma flow with the expanding supersonic flow. In the slab target the sonic point is singular. No steady supersonic flow is connected with the deflagration wave in the slab target. The singularity at the sonic point disappears in the spherical target when the beam pressure is in the balance with the pressure of the plasma in the spherical configuration.

Acknowledgement

This work was partly supported by the Scientific Research Fund of the Ministry of Education, Science and Culture in Japan.

References

1) S. Mikoshiba and B. Ahlborn: Phys. Fluids 17 (1974) 1198.

2) T. Abe, K. Kasuya, K. Niu and M. Tamba: J. Phys. Soc. Japan (submitted).

3) H. Takabe et al: J. Phys. Soc. Japan 45 (1978) 2001.

4) T. Miyamoto: Kakuyugo no tameno Plasma Butsuri (Iwanami, Tokyo, 1976) [in Japanese].

Figure Captions

Fig.1. A schematic diagram of a target and ion beams.

Fig.2. A structure of a deflagration wave. a) A profile of the plasma temperature. b) A profile of the plasma velocity. c) A profile of the beam velocity. These curves are drawn for $\alpha^2\beta = 0.025$, $\alpha^3\beta = 2.5$.

Fig.3. The ratio of the beam velocity at the sonic point to that at the infinite point. Two curves are plotted against $\alpha^3\beta$ for $\alpha=10$ and 100.

Fig.4. The ratio of the length $\bar{\lambda}_s$ of the deflagration wave in the spherical target to the length $\bar{\lambda}_s'$ in the slab target. Two curves are plotted versus $\alpha^3\beta$ for $\alpha=10$ and 100.

Fig.5. The strength of the deflagration wave versus $\alpha^3\beta$. a) The ratio T_f/T_s of the temperature. b) The ratio u_s/u_f of the number density. The corresponding ratios in the slab target are shown by dotted lines.

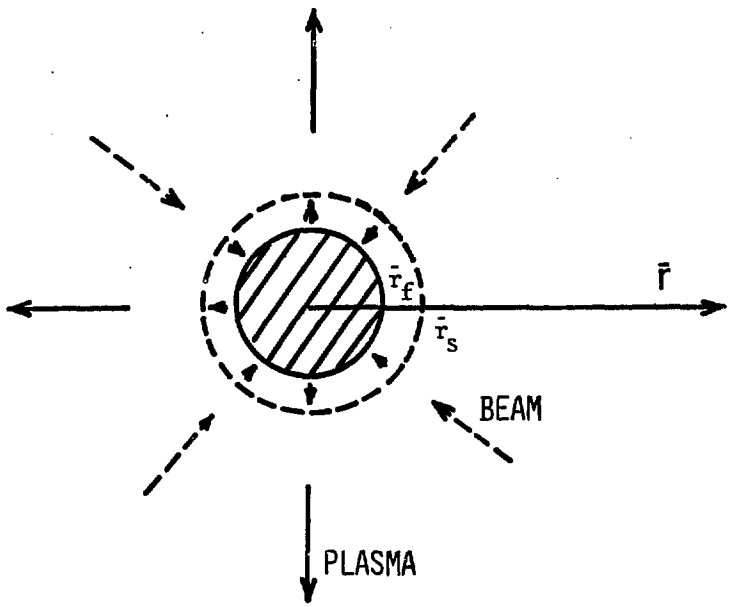

FIG. 1

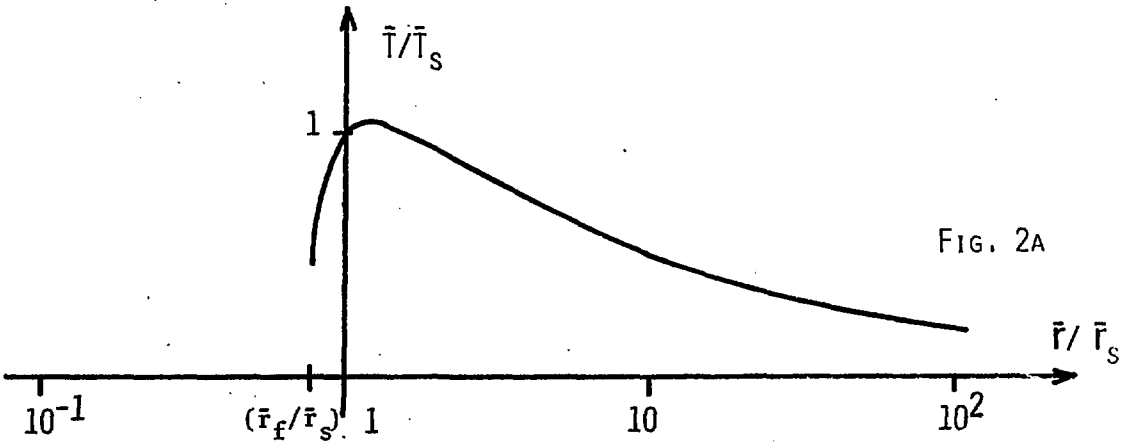

FIG. 2A

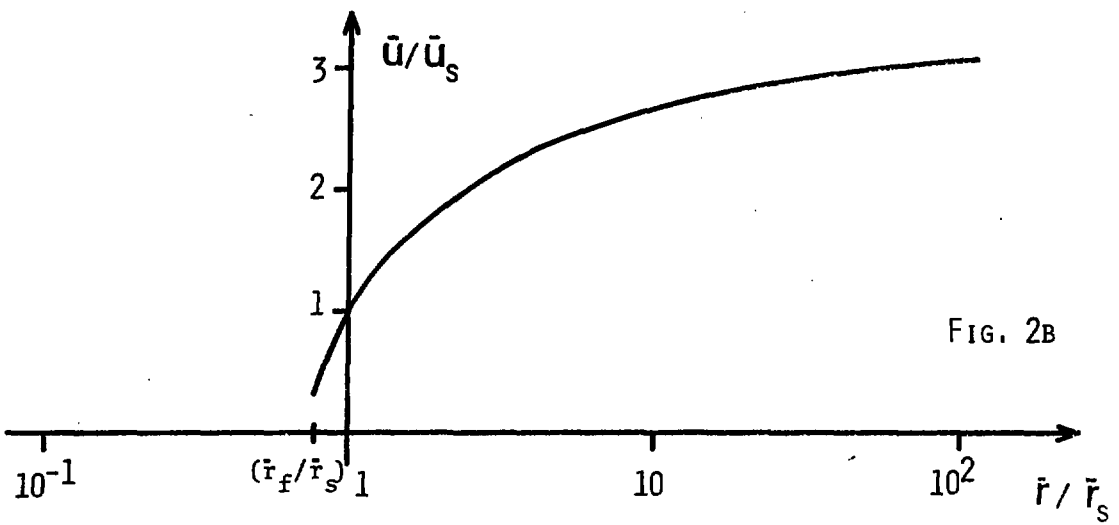

FIG. 2B

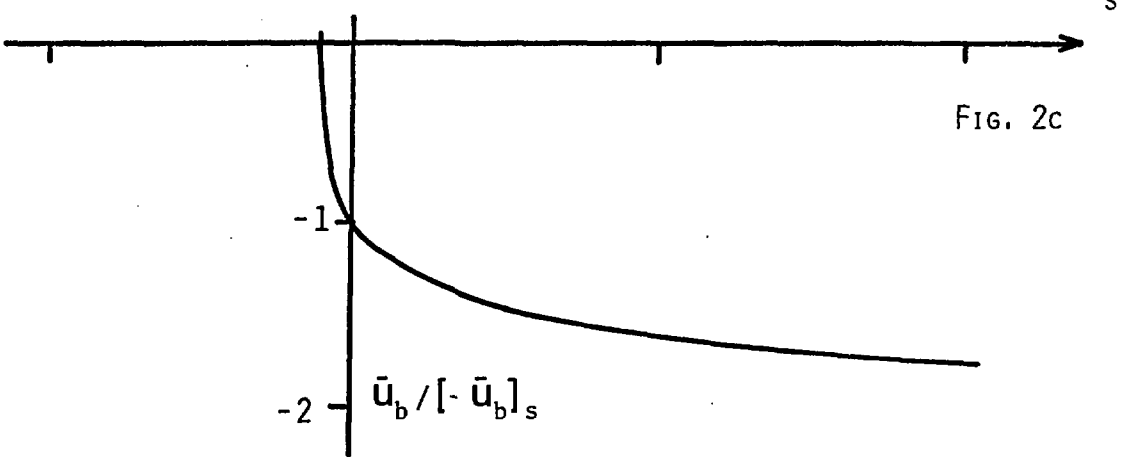

FIG. 2C

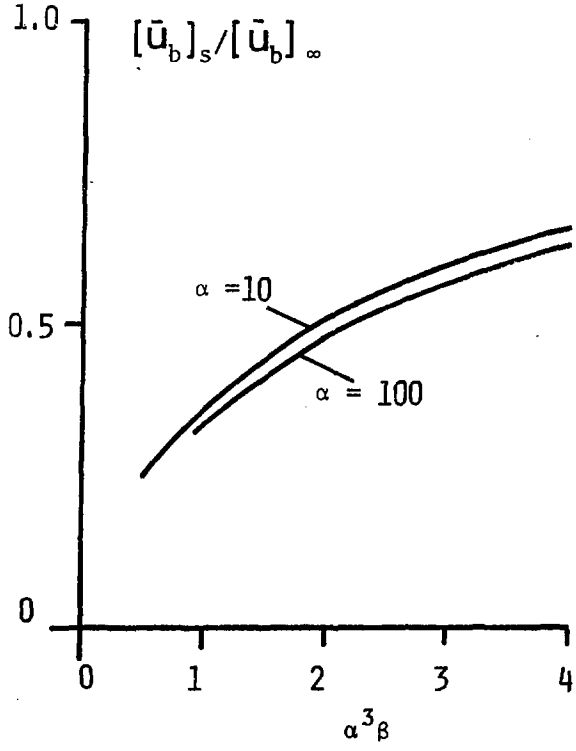
1.0
$[\bar{u}_b]_s/[\bar{u}_b]_\infty$
0.5
0
α =10
α = 100
0
1
2
3
4
$\alpha^3\beta$

FIG. 3

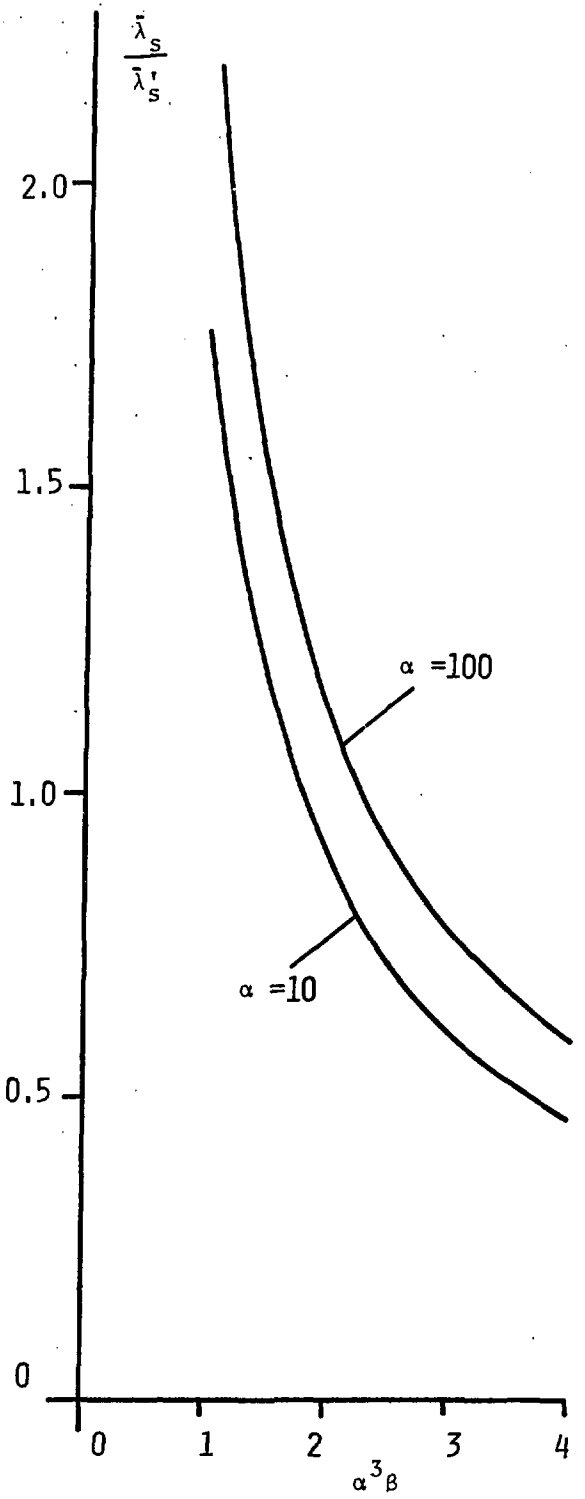
$\frac{\bar{\lambda}_s}{\bar{\lambda}'_s}$
2.0
1.5
1.0
0.5
0
α =100
α =10
0
1
2
3
4
$\alpha^3\beta$

FIG. 4

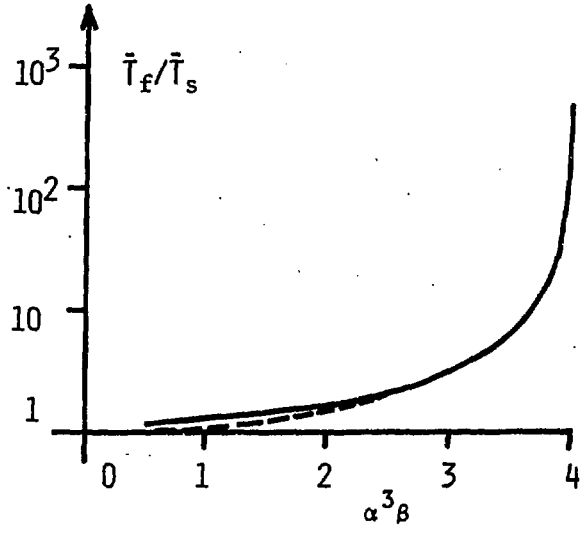
10^3
$\bar{T}_f/\bar{T}_s$
10^2
10
1
0
1
2
3
4
$\alpha^3\beta$

FIG. 5A

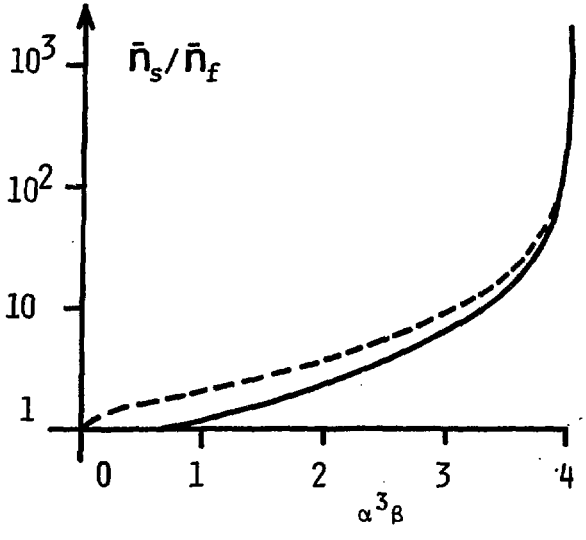
10^3
$\bar{n}_s/\bar{n}_f$
10^2
10
1
0
1
2
3
4
$\alpha^3\beta$

FIG. 5B